2
Review of Literature

Microwave spectrum is divided in different frequency bands viz. L (1-2 GHz), S (2-4 GHz), C (4-8 GHz), X (8-12 GHz), Ku (12-18 GHz), K (18-26.5 GHz) etc. The different frequency bands have applications in various fields including stealth, transmission, communication, electronics etc. Among these areas, MW stealth technology has gained significant research interest due to its strategic applications in the defence sector. The back reflected MW power towards the receiver direction, quantify the overall contribution of absorption, transmission, specular reflection, and scattering in other directions. In the process of microwave absorption/ reduction of RCS, the aim is to minimize the back-reflections of MW signals and maximize the absorption of MW signal within the materials itself. In this chapter, a theoretical framework has been given for MW absorption mechanism inside the materials as well as necessary conditions to minimize the back reflection of MW radiation as well the criterion for selection of different class of materials for efficient MW absorption.

2.1 MW Loss Mechanisms

The propagation of EM wave in materials medium is governed by Maxwell Equations [Griffiths, 1999] as given below Eqs. (2.1)-(2.4)

$$\nabla . \boldsymbol{D} = \rho_f \tag{2.1}$$

$$\boldsymbol{\nabla} \times \boldsymbol{E} = -\frac{\partial \mathbf{B}}{\partial \mathrm{t}} \tag{2.2}$$

$$\nabla . \boldsymbol{B} = 0 \tag{2.3}$$

$$\boldsymbol{\nabla} \times \boldsymbol{H} = \boldsymbol{J}_f + \frac{\partial \mathbf{D}}{\partial \mathrm{t}} \tag{2.4}$$

Where **D** is the electric displacement vector responsible for polarization in materials, ρ_f is free electron charge density, **E** and **B** are electric and magnetic field vectors of EM wave, **H** is magnetic field strength, $\boldsymbol{J}_f$ is free electron current density. The time varying electric field vector **E (z,** t**)** = $\mathbf{E}_0 e^{-i(kz-\omega t)}$ and magnetic field vector **B (z,** t**)** = $\mathbf{B}_0 e^{-i(kz-\omega t)}$ interact with matter as shown in Figure 2.1, schematically. The electric and magnetic field vectors will change depending upon nature of available static or moving charges.

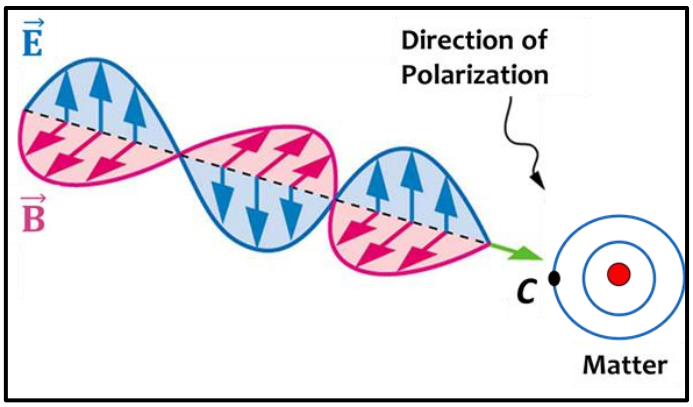

Figure 2.1 : Interaction of EM wave with matter

The interacting microwaves can be absorbed under following conditions:

(i) If the incident energy is equivalent to the electronic energy gaps (e.g. electronic, vibrational, or rotational).
(ii) The electronic vibrations are in coherence with the incident wave frequencies.
(iii) The dipolar relaxation with incident electromagnetic waves.
(iv) The magnetic domain relaxation with incident electromagnetic waves.

The material's parameters such as electrical permittivity, magnetic permeability and electrical conductivity will essentially determine the nature of interaction of EM waves with the material. This nature of interaction will govern the reflection, transmission and absorption of incident EM radiation. The microwaves, which are part of EM spectrum, have characteristics transmission (penetration through non-lossy insulators), reflection (from conducting surface due to presence of free electrons), absorption (lossy medium or non-lossy medium with suspended MW lossy particulates) as summarized in Figure 2.2, schematically.

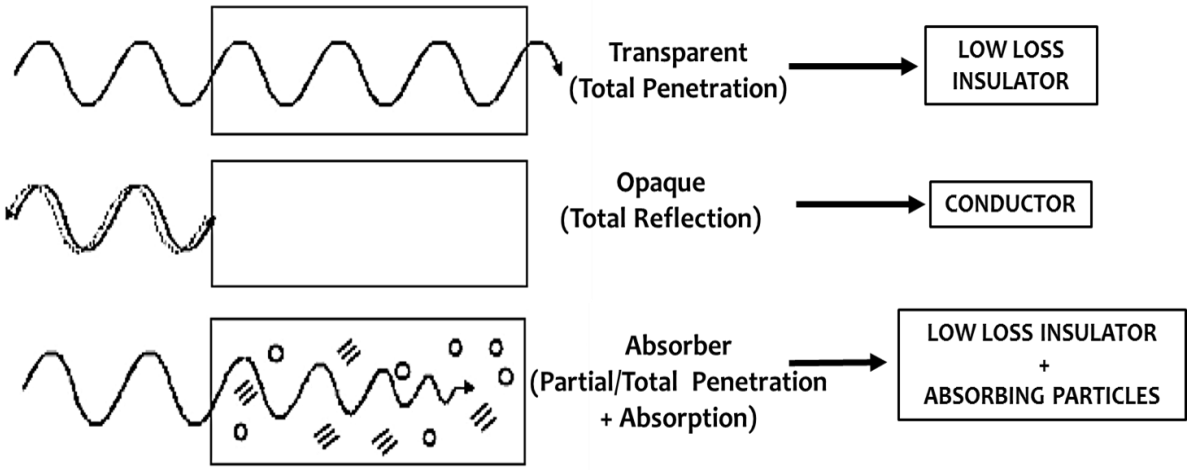

Figure 2.2 : Microwave interaction with different mediums (Source: Sutton, 1989)

2.1.1 Impedance Matching Criterion

The reflection of microwaves occurs when it encounters change of medium in its travel path. This reflection is represented by reflection coefficient R_{coe}. In case of a wave entering into a material medium from free space, the R_{coe} is given by the relation, $R_{Coe} = \frac{Z_m - Z_0}{Z_m + Z_0}$, where $Z = \sqrt{\frac{\mu_m}{\varepsilon_m}} = Z_0\sqrt{\frac{\mu_r}{\varepsilon_r}}$ is impedance of materials having permittivity ε_m and permeability μ_m and $Z_0 = \sqrt{\frac{\mu_0}{\varepsilon_0}} \sim 377$ Ω is free space impedance.

In ideal situations, the impedance of materials medium (Z_m) should be equal to the free space impedance Z_0 resulting into, $\mu_r = \varepsilon_r$, and thus, causing no reflection from the front surface ($R_{Coe} = 0$) as shown in the Figure 2.3(a) [Gaylor, 1989]. However, such Z-matched materials and absorber designs are rarely available. If the material with close approximation of Z-matching is exposed to the MW signals, the waves will enter inside the material and reflected back from any interior metallic surface available within the objects as shown in Figure 2.3(b). For example, in the case of aircrafts, even if the fuselage design is non-reflecting due to curved geometry, the MW signals will be reflected back from the metallic engine part as shown in Figure 2.3(c), schematically. Therefore, the impedance matching at interfaces of material layer is not the only criterion to reduce the MW back reflection in the receiver direction. Thus, it is important to design effective microwave absorber systems for stealth application.

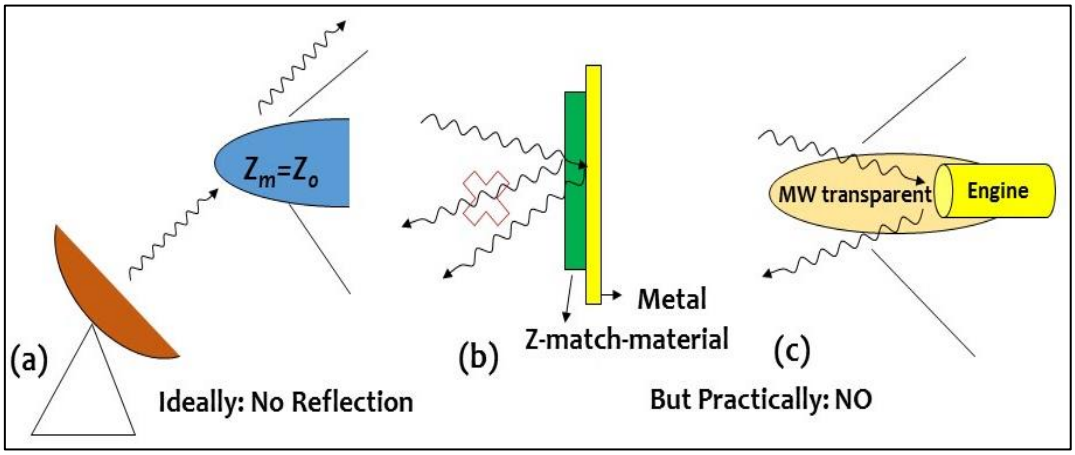

Figure 2.3 : Reflection mechanism of MW signals from metallic and non-metallic surfaces

2.1.2 Microwave Losses in Materials

The propagation of MW signals inside the materials is governed by indices of refraction (n) between the free space and lossy materials, as given by [Saily and Raisanen, 2003] relation $n = \frac{k}{k_0} = \sqrt{\mu_r^* \varepsilon_r^*}$, where $\varepsilon_r^* = \varepsilon_r' - j\,\varepsilon_r''$ and $\mu_r^* = \mu_r' - j\,\mu_r''$ are the complex relative electrical permittivity and magnetic permeability respectively and k is wave propagation vector. The effective refractive index of lossy materials assists in absorbing the MW signals, once entered inside the material because of the relaxation of magnetic domains or matching frequencies in the desired frequency range. Further, the suspension of absorbing particulates also assists in multiple scattering of MW signals inside the materials as shown schematically in Figure 2.4. The real part of permittivity and permeability depicts the energy storage efficiency due to their electric or magnetic field vectors, respectively. It is the imaginary component of these quantities that accounts for the loss in the material.

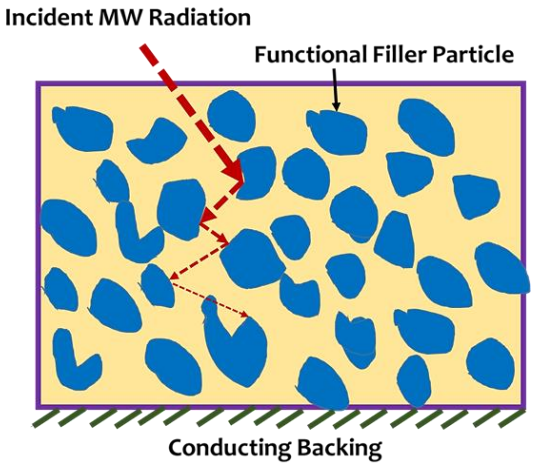

Figure 2.4 : Interaction of MW signals with MW absorbing Materials (Source: Hernandez *et al*.)

The MW power is attenuated exponentially exp (-α x), where α is attenuation coefficient given by Eq. (2.5) [Saville, 2005]

$$\alpha = -\sqrt{\mu_0\,\varepsilon_0}\,\omega(a^2+b^2)^{\frac{1}{4}}\sin\left(\frac{1}{2}tan^{-1}\left(-\frac{a}{b}\right)\right) \qquad (2.5)$$

Here a, b coefficients are given as $a = \left(\varepsilon_r'\,\mu_r' - \varepsilon_r''\,\mu_r''\right)$, $b = \left(\varepsilon_r'\,\mu_r'' + \varepsilon_r''\,\mu_r'\right)$.

Thus, the materials parameters ε_r', μ_r', ε_r'' and μ_r'' must be large to realize the larger attenuation coefficient α. The characteristics of MW interaction are different in dielectric and magnetic materials because of the different loss mechanisms and different MW frequency dependence in these materials. The MW loss mechanisms are discussed below for both types of materials.

2.1.2.1 Dielectric Losses in Materials

A dielectric is a medium where the charged particles will polarize under an external electric field. The net polarization (**P**) in such materials depend on the applied field (**E**), electric susceptibility (χ_e), and displacement vector **D**, which can be represented in terms of permittivity and electric filed vectors as given in Eqs. (2.6)-(2.7)

$$\boldsymbol{P} = \varepsilon_0 \chi_e \boldsymbol{E} \tag{2.6}$$

$$\boldsymbol{D} = \varepsilon_0 \boldsymbol{E} + \boldsymbol{P} = \varepsilon_0 (1 + \chi_e) \boldsymbol{E} = \varepsilon_0 \varepsilon_r^* \boldsymbol{E} \tag{2.7}$$

When time varying electric field $\mathbf{E(z,t)} = \mathbf{E_0}\, e^{-i(kz-\omega t)}$ passes through a dielectric material, the effective electric field generated within the material tries to align the dipoles in the direction of field during the positive and negative half cycles of the electrical field. The dipoles may follow the electric field variation at lower frequencies and be in coherence. However, at microwave frequencies, the alignment of diploes does not follow the frequency of EM fields because of their relatively large relaxation time. The diploes lose their energy interacting with the external field because of the resistance faced by frictional and elastic forces in the material during relaxation. The real and imaginary permittivity parameters exhibit dispersion characteristics, which can be understood in terms of Debye relations, given in Eq. (2.8) and (2.9) [Kittel, 2004].

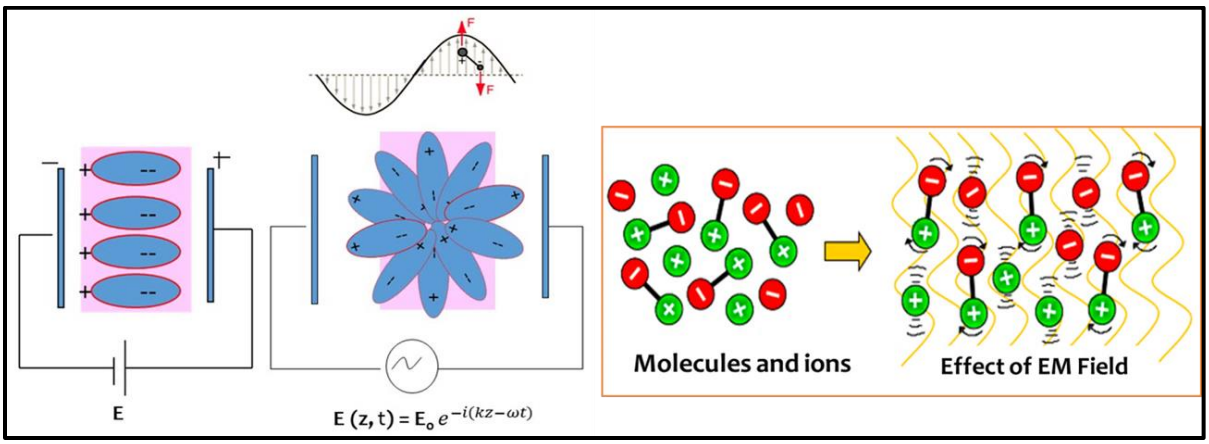

Figure 2.5 : Dielectric relaxation mechanism with incident EM radiation

$$\varepsilon'(\omega) = n^2 + \frac{\varepsilon(0) - n^2}{1 + \omega^2 \tau^2} \tag{2.8}$$

$$\varepsilon''(\omega) = \frac{\varepsilon(0) - n^2}{1 + \omega^2 \tau^2}\, \omega\tau \tag{2.9}$$

Where ω is frequency of EM radiation, $\varepsilon'(\omega)$ and $\varepsilon''(\omega)$ are frequency dispersive real and imaginary parts of the permittivity, τ is relaxation time, ε (0) is the permittivity value at ω=0. The dielectric loss term $\varepsilon''(\omega)$ shows maxima at resonance conditions (ω ~1/τ). The dielectric loss tangent $\tan\delta_e$ is also commonly used to describe these losses, which is defined by Eq.(2.10)

$$\tan\delta_e = \frac{\varepsilon_r''}{\varepsilon_r'} = \frac{\sigma}{2\pi\, \varepsilon_0\, f \varepsilon_r'} \tag{2.10}$$

Where σ is total effective conductivity (S/m) caused by ionic conduction/displacement currents, f is frequency of incoming MW signals and ε_r' is real part of relative permittivity. The dielectric loss tangent also depends on real part of relative permittivity and conductivity (σ) of the material. Loss tangent values ($\tan\delta_e$) increase with σ and ε_r', provided the conditions of impedance matching at material's surface e.g. in case of metals, σ and ε_r' are extremely high, which may cause the maximum reflection of the MW signals. Therefore, to attain the optimal loss tangent values, there is always a trade-off between conductivity and real part of the permittivity and therefore

the material's parameters should be engineered to achieve the effective loss tangent over the desired frequency range.

2.1.2.2 Magnetic Losses in Materials

The magnetic class of materials consists of microscopic atomic magnetic dipoles arising from the unpaired electrons spin moment and their complex interaction. The magnetization of materials can be manipulated by external magnetic field bias, which strongly depends on the complex permeability μ* of the materials given in Eq.(2.11)

$$\boldsymbol{B} = \mu^* \boldsymbol{H} = \mu_0 \mu_r^* \boldsymbol{H} = \mu_0(\boldsymbol{H} + \boldsymbol{M}); \boldsymbol{M} = \boldsymbol{H}(\mu_r^* - 1) \quad (2.11)$$

Where **B** is the magnetic flux density, **H** is the magnetic field intensity, **M** is the magnetization, μ_0 is the permeability of free space and μ_r^* is real part of complex relative permeability. For small fields, the magnetization is proportional to the field intensity. Further, μ_r^* can be expressed as given in Eq.(2.12)

$$\mu_r^* = \frac{\mu}{\mu_0} = 1 + \frac{\boldsymbol{M}}{\boldsymbol{H}} = 1 + \chi_m \quad (2.12)$$

In the magnetic materials, the unpaired electrons provide spin magnetic movement ($\boldsymbol{\mu_s}$) expressed by the relation $\boldsymbol{\mu_s} = -g_s \left(\frac{e}{2m}\right) \boldsymbol{s}$, where g_s is spin splitting factor (has value equals to 2), the $(\frac{e\hbar}{2m})$ is Bohr Magneton (μ_B) having value 9.272 x 10^{-24} Am^2 and **s** is spin vector. The spin magnetic movement ($\boldsymbol{\mu_s}$) experiences a torque under the magnetic field (due to net magnetization of materials) and it precesses around the direction of magnetic field. The frequency of precession is known as Larmor angular frequency f_L and is given by a relation [Moulson and Herbert, 2003] $f_L = \frac{\gamma \mu_0}{2\pi} \boldsymbol{H}$, where $\gamma = \frac{g\mu_B}{h}$ is gyroscopic ratio and **H** is net static/dynamic magnetic field. In external time varying magnetic field $\mathbf{H(z,t)} = \mathbf{H}_0 e^{-i(kz-\omega t)}$, the precessional motion further enhances at resonant frequency f_L as shown in Figure 2.6 (a). The precession of magnetic moment will be dissolute during the relaxation process. In the realistic conditions, the spin-lattice coupling will again be responsible for damping of the precessional motion of magnetic moment. Therefore, the incident MW signals are attenuated due to spin resonance relaxation process, known as Ferromagnetic Resonance (FMR) relaxation.

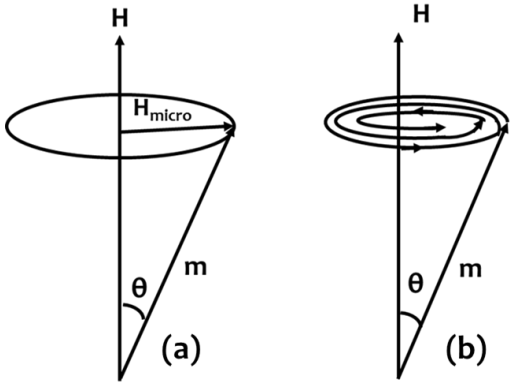

Figure 2.6 : Spin resonance relaxation mechanism (a) Precession under the influence of external magnetic field (b) Dissipation of EM signal

Another relaxation mechanism associated with magnetic materials is the relaxation of domain walls with EM signals at GHz frequency range. The domain walls in a magnetic material consist of segments of unpaired spins aligned in same directions, providing a uniform direction of magnetization for a domain. The domains present in the magnetic materials will try to align in the direction of external field with a small marginal displacement of domain walls, leading to the respective lattice distortions. The energy gained from external MW radiation is attenuated in such domain wall motion in terms of inertial heat loss. For the sinusoidal MW signals, the equation the domain wall motion can be expressed by the following Eq. (2.13)

$$m\ddot{x} + \beta\dot{x} + kx = 2M_s B(t) \quad (2.13)$$

Where x is the domain wall displacement with respect to its normal, m is the domain wall inertia, β is the damping constant, k is the coefficient of stiffness, M_s is saturation magnetization and B(t) is time varying magnetic field. This equation is similar to the damped harmonic oscillator with resonance frequency $\omega = \sqrt{\frac{c}{m}}$ for small damping. The domain wall relaxation dominates at lower frequencies ~1-2 GHz. However, at relatively higher GHz frequencies, the domain wall motions could not follow the external time varying magnetic field. The losses caused by FMR relaxation follows the high frequency EM radiation and hence, causing MW losses at higher frequencies. Thus, the losses from the spin and domain wall relaxation under the time varying magnetic field $\mathbf{B}(z,t) = \mathbf{B}_0 e^{-i(kz-\omega t)}$ are analogous to the dielectric losses under the time varying electric field. The unpaired spin's contribution to the MW losses is quantified by the magnetic loss tangent ($\tan\delta_m$) defined by $\tan\delta_m = \frac{\mu_r''}{\mu_r'}$, where μ_r' and μ_r'' are real and imaginary part of relative permeability of the material.

From the foregoing discussions, it is clear that both the dielectric and magnetic materials can be used for the design and development of microwave lossy mediums. Although the loss mechanisms are of different origins in these materials, both absorb the EM energy, followed by heat dissipation in the system. The main objective of the thesis work is to design and tailor the material's EM parameters, responsible for MW absorption over the wide MW frequency range.

2.1.3 EM Absorption on Single Layer Microwave Absorber (Dallenbach Layer)

A schematic viewpoint of a single layer MW absorber with conducting backing is shown in Figure 2.7. A representative electromagnetic interaction mechanism is also explained. For a close approximation, the conducting backing substrate is assumed to be a Perfect Electrical Conducting (PEC) to ease the computational studies for MW absorption. Firstly, the free space incoming MW signal gets partially reflected from the top absorber layer, due to certain amount of impedance mismatch (as total impedance matching is an ideal case). The effective wavelength of the MW signal inside the material is λ_m, given as $\lambda_m = \frac{\lambda_0}{\sqrt{|\mu_r^*||\varepsilon_r^*|}}$ where λ_0 is free space wavelength of MW signal, ε_r^* and μ_r^* are complex permittivity and permeability, respectively.

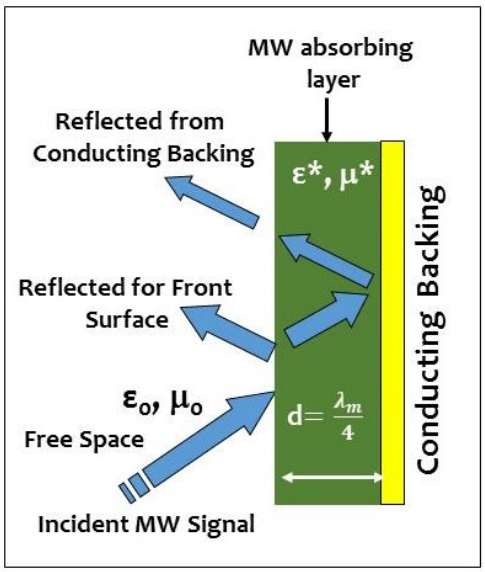

Figure 2.7 : Interaction of MW with single layer absorber with conducting backing

Secondly, the MW signal, inside the lossy materials, gets attenuated, depending upon the nature of material used as an absorber. The MW signal wave is back reflected again at the conducting backing substrate and MW absorber interface due to the high conductivity of substrate in general. The thickness of the absorber i.e. the path length of MW signal is chosen as quarter wavelength, to introduce a path difference of $\lambda/2$ between front surface reflected and conducting backing reflected MW signals. This intentionally created $\lambda/2$ path difference will assist in minimizing any reflected MW signal because of the destructive interference between these reflected signals. The scheme for such quarter wavelength structure was first proposed by Dallenbach and Kleinsteuber [Dallenbach and Kleinsteuber, 1935] and thereafter, such MW absorber structures are popularly known as Dallenbach layer. The input impedance of incident wave, entering inside the material (Z_1), is given by following Eq. (2.14)

$$Z_1 = Z_m \tanh(\gamma d) \tag{2.14}$$

Where, Z_m is the characteristic impedance of the material as defined earlier, d is the thickness of the MW absorbing layer, γ is the propagation constant, which is a complex quantity and is given by following relation [Eq. (2.15)]

$$\gamma=\alpha+\beta j = \frac{j2\Pi}{\lambda_0}\sqrt{\mu_m^*\varepsilon_m^*} \tag{2.15}$$

The normalized (with respect to free space) input impedance for an incident MW signal is given by Eq. (2.16)

$$\eta = \sqrt{\frac{\mu_r^*}{\varepsilon_r^*}} tanh\left(\frac{j\,2\pi d}{\lambda_0}\sqrt{\mu_r^*\varepsilon_r^*}\right) \tag{2.16}$$

The phase of front layer and conducting backing reflected waves depends on ε, μ and d, while their relative amplitudes depend on the MW losses in the material. The normalized reflection coefficient may be represented as given in Eq. (2.17)

$$R_N = \frac{\eta-1}{\eta+1} = \frac{\sqrt{\frac{\mu_r^*}{\varepsilon_r^*}} tanh\left(\frac{j\,2\pi d}{\lambda_0}\sqrt{\mu_r^*\varepsilon_r^*}\right)-1}{\sqrt{\frac{\mu_r^*}{\varepsilon_r^*}} tanh\left(\frac{j\,2\pi d}{\lambda_0}\sqrt{\mu_r^*\varepsilon_r^*}\right)+1} \tag{2.17}$$

Further, the reflection loss (R.L.), which quantifies the net power reflected back in the receiver direction, is represented in decibel (dB) and is given by R.L. (dB) = $-20\log_{10}|R_N|$. These relations for input impedance and reflection coefficient clearly suggest that in order to achieve the maximum return loss, the material should possess both high values of complex permittivity and permeability. However, a relatively higher value of one of the parameters over the other will lead to a discontinuity between free space and lossy surface due to the large impedance mismatch between them. This phenomenon leads into large reflections of the electromagnetic radiations. Further, to obtain the minimum back reflections at wave impedance matching, the absorber thickness will be comparable to quarter wavelength of MW signal inside the material ($\lambda_m/4$). In this case, the reflection loss will be the maximum and the loss profile will be confined in a narrow band. It can be expressed as $R_N = \frac{\eta-1}{\eta+1} = 0$ with the matched thickness (d_m) given as

$$d_m = \frac{c}{4f\sqrt{|\mu_r^*||\varepsilon_r^*|}} \tag{2.18}$$

Thus, it is evident that the MW absorption at lower frequencies (~1-8 GHz) will require relatively higher thickness as compared to that for high frequency range (8-18 GHz). The dielectric materials are mostly suitable for the 8-18 GHz frequency range with realistic absorber thickness, as the thickness requirement for these materials is very high for the lower frequency range 1-8 GHz (due to absence of characteristics losses in this range). Therefore, magnetic materials are better choice as MW absorbing filler material in 1-8 GHz frequency range as a number of ferrite and other magnetic systems show the phenomenon of ferromagnetic resonance in this frequency range. These limitations of magnetic and dielectric materials compel to develop

novel class of multifunctional materials, where both magnetic and dielectric loss mechanisms may be combined to realize the MW absorber for entire 1–18 GHz frequency range.

Considering the complex radiation-matter interaction, the performance of MW absorbing products, in form of coating/sheet/structures, have combined effect of materials performance parameters, their dispersion in host matrix and the designed thickness of absorber layer. The observed reflection loss (R.L.) in such structures has the cumulative effect on MW loss, and quantification of individual component's MW loss contribution is extremely difficult. The objective of the thesis work is to synthesize dielectric, magnetic and magneto-dielectric materials with desirable electrical permittivity, magnetic permeability and electrical conductivity values and their use in the form of lossy absorber while minimizing the impedance mismatch to maximize the reflection loss. The details of synthesis techniques, commonly used for such materials, are described in the following section.

2.2 Synthesis Techniques for Microwave Absorbing Materials

MW absorbing materials are being synthesized by physical, chemical and mechano-chemical techniques. However, to produce in bulk with reproducible material's properties, chemical and mechano-chemical methods are being widely used. In this section, we will briefly discuss about various physical, chemical and mechano-chemical methods for the synthesis of different MW absorber materials viz. Ni-Zn spinel ferrites, graphite coated Ni nanoparticles, tetragonal phase $BaTiO_3$ powder, $BiFeO_3$ multiferroic material and Z-type Sr hexaferrites. The opted synthesis techniques can be scaled to produce the materials in bulk with desired functional properties for MW absorption applications.

2.2.1 Sol-gel Technique

Sol-gel method is a common technique to prepare ceramics and glasses since decades and now being used for synthesis of metal oxides and other nanomaterials due to its ability to control the reaction parameters [Gottardi,1982; Brinker *et al.*, 1994; Schmidt *et al.*, 1998]. In this process, hydrolysis of reactive precursors, preferably metal alkoxides, nitrate, chlorides etc., is done in presence of chelating agents viz. acetylacetone (ACAC), citric acid, ethylene glycol etc. which promote the gelation process. Ultrafine powder of metal hydroxide is obtained during the condensation of corresponding hydroxide molecules after removing the residual water, followed by drying. The obtained cross-linked structure (xerogel) is further heated to get the respective metal oxides. The sol-gel method has advantages over other synthetic routes as it involves relatively low-temperature processing of materials, prevents the uniformity of shape and size of the final product, and most importantly, is a low cost process, which can be scaled for large production without any difficulty [Sui and Charpentier, 2012]. Cerena prepared tetragonal $BaTiO_3$ powder by hydrolysis/condensation of alkoxide precursor and acac: $Ti(OR)_4$ chelating agent followed by initial heating at 100°C and later annealed at 1000°C [Cernea, 2005]. Fu *et al.* have used bismuth nitrate and iron nitrate as precursors for the preparation $BiFeO_3$ ferrite powder using C_2H_5OH and nitric acid as chelating agents. The phase pure powder has been synthesized after annealing at 600°C for 1h [Fu *et al.*, 2012]. Sol-gel method has been used by many research groups for the preparation of Ni spinel ferrite [Chen and He, 2001], Cr_2O_3 [Znaidi and Pommier, 1998], MgO [Chhor *et al.*, 1995] etc.

2.2.2 Solvo-thermal/Hydrothermal Method

Hydrothermal or solvo-thermal method is used for the synthesis of complex metal oxides by precipitation of salt precursors under restricted conditions of high temperature and pressure in solution phase, which is usually not possible in common sol-gel process. The reaction is suitable for reactants, which otherwise are not soluble in water at normal temperature (<100°C) and pressure conditions (<1atm). The solvo-thermal reactions are performed by dissolution/suspension of reactants in optimized quantity of water in closed vessels at high temperature up to 300°C and high pressure conditions (<20MPa) in acid digester reactors or

autoclaves, to achieve the supercritical stage of water in the vessel. Further, the supercritical stage of water provides preferable conditions for reaction to convert the reactants into the final product [Hayashi, H. and Hakuta, 2010]. The advantages of hydrothermal process include energy efficient green synthesis, high purity of the end product, precise control on crystallite size and morphology etc. [Komarnenia *et al.*, 2010]. The hydrothermal process has been widely used for preparing variety of metal oxides, titanates and phosphates. Narrow size distribution of barium titanate nanocrystals was achieved using hydrothermal method in the presence of surface modifier to restrict the further growth of nano-crystalline material [Lu *et al.*, 2000; Lee *et al.*, 2012; Park *et al.*, 2002]. Various oxides viz. ZnO [Ohara *et al.*, 2004; Sue *et al.*, 2004], $CoFe_2O_4$ [Cote *et al.*, 2003], Al_2O_3 [Sato *et al.*, 2008], ZrO_2 [Becker *et al.*, 2008] etc. have also been prepared with proper stoichiometry under controlled reaction conditions using hydrothermal process and thus, may be a very useful synthesis process for designing materials with desired uniformity of the shape and size of the synthesized materials.

2.2.3 Chemical Co-precipitation

Chemical co-precipitation method is a simple, cost effective, and energy efficient synthesis technique to prepare metal/ceramic/semiconductor oxides. In this process, initially the aqueous solution of salt precursor (metal chlorides/nitrates) is prepared in proper stoichiometry. These aqueous solutions are further precipitated in the water medium with the help of $NaOH/NH_4OH$ alkali solutions. The precipitated metal hydroxides are washed with hot water to remove residual impurity ions, followed by filtration and drying to obtain resultant powder. The resulted powder is calcined at high temperature with optimized thermal cycles to get the desired phase pure oxides materials. $Ni_{1-x}Zn_xFe_2O_4$ spinel ferrite nanoparticles were prepared by precipitation of aqueous solution of nickel, iron and zinc salt precursor using NaOH solution, followed by high temperature annealing [Azhagushanmugam *et al.*, 2013; Velmurugan *et al.*, 2010]. Various metal oxides viz. Fe_2O_3 [Wang *et al.*, 2013; Kandpal *et al.*, 2014; Petcharoena and Sirivat, 2012] are also synthesized successfully using this technique.

2.2.4 Polymer encapsulated Nanoparticles

To synthesize the nanomaterials, polymer can act as a host matrix to achieve an effective control over particle size and shape while restricting particle growth in polymer chains. The polymer encapsulated metal/metal oxide can be prepared either by in-situ reduction of metal particles or intercalation of metal particles in polymeric matrix [Oliveira and Machado, 2013; Schmidt and Malwitz, 2003; Niasariand Ghanbari, 2011; Hanemann and Szabo, 2010]. The synthesis process allows very good dispersion, control and organized growth of inorganic nanomaterials in polymeric complex. The annealing of these metal doped polymer nanocomposites in an inert ambient converts the materials into core-shell geometries with carbon/graphitic shell over metal cores. Metal/metal oxides nanoparticles such as Ag [Panacek, 2006], $CoFe_2O_4$ [Ahmed and Kofinas, 2002], Fe_3O_4 [Gass*et al.*, 2006], PbS [Lu *et al.*, 2005] etc. have been prepared in suitable polymeric/co-polymer matrices [Folarin *et al.*, 2011] and the process can be used for other such systems as well.

2.2.5 Precursor Method

This method uses non-aqueous precipitation of metal ions using precipitant solutions (oxalic acid/citric acid) using a solid state reaction. The decomposition of corresponding solid compounds (oxalate/citrate) provides the end product following its calcination at high temperature. This method provides highly homogeneous end products with high purity and is very useful to get ferrite powders with uniform/homogeneous phase at relatively low processing temperatures. Ni-Zn spinel ferrites powders with different compositions were prepared by different research groups converting the Ni, Zn and Fe reactants in Ni-Zn oxalate precursor $Ni_XZn_{1-X}Fe_2(C_2O_4)_3.nH_2O$ followed by heat treatment at high temperatures [Chaudhari *et al.*, 2010; Sarangi *et al.*, 2010]. Arya *et al.* prepared nano barium lead titanate ($Ba_xPb_xTiO_3$) using citrate precursor route wherein precipitation of barium carbonate and lead nitrate is carried out in presence of ethylene glycol and citric acid [Arya *et al.*, 2003]. Various perovskite and metal oxide

materials viz. barium strontium titanate ($Ba_{1-x}Sr_xTiO_3$) [Khollam *et al.*, 2005; Li *et al.*, 2008], Cuo, ZnO, Fe_3O_4 [Ahmad *et al.*, 2011; Lagashetty *et al.*, 2007], $BaFe_{12}O_{19}$ [Mohsen, 2010] etc. were synthesized by precursor route.

2.2.6 Arc-Discharge Method

Arc-discharge method is a physical method, widely used for preparation of graphite, CNT, carbon/graphite coated metal nanoparticles etc. In this method, electrodes of desired materials are used as cathode and anode, in a vacuum chamber in conjunction with suitable substrates to collect the final material. An inert gas, preferably high purity He/Ar gas, is filled in the chamber at optimized pressure and arc is generated with the help of constant DC power supply. A cathode is made of carbon/graphite and the high purity metal/alloy is taken at anode position to synthesize the carbon/graphite coated metal/metal alloy nanoparticles, [Fang *et al.*, 2015]. Han *et al.* prepared $NiFe_2O_4$ nanoparticles as core materials covered with onion like carbon shell by annealing of FeNi/C nanoparticles obtained by arc-discharge method [Han *et al.*, 2015]. Carbon nanotubes were prepared by Ando and Zhao using the arc-discharge method wherein both anode and cathode were made of graphite and synthesized CNTs were collected from the cathode [Ando and Zhao, 2006]. Similarly, core-shell structures of MoS_2 [Alexandrou *et al.*, 2013]; Al-Si/C [Tulugan *et al.*, 2013], Fe/C [Shen *et al.*, 2015] etc. have been investigated using the arc-discharge method.

2.2.7 Self Propagation High Temperature Synthesis (SHS)

The SHS technique is a single step process to prepare ceramics, refractory materials, chalcogenides, metal oxides, intermetallics and nanomaterials using exothermic reaction among initial precursors [Pampuch, 1993; Padyukovand Levashov, 1993; Merzhanov, 2004]. The proper stoichiometric mixture of reactants is homogenized with an explosive agent in optimized concentration in a specially designed an SHS reactor. The high temperature reaction is initiated with using either an initial spark triggered by electric arc, or a flame or a laser. The high temperature combustion thermal energy propagates from a hot zone to the cold zone, and thus assisting the conversion of starting precursors into the desired product at high temperature of ~3000K [Bowen and Derby, 1997]. The energy required for self-propagation in such reactions is attained from in-situ exothermic heat produced during the reaction process. To avoid the oxygen deficiency during the combustion process, additional controlled oxygen feeding may be integrated during the reaction. The advantages of this method include the instant voluminous production of end product without prolonged heating of precursors, removal of volatile impurities, high conversion ratio of end product, and the choice of economic raw precursor etc. However, there is a less control on the reaction parameters, once ignition reaction has started. The thermodynamic processes, related to such exothermic heat release and propagation of reaction need to be understood for each class of materials. Various materials viz. thermoelectric Cu_2Se [Su *et al.*, 2014], hexaferrites $Ba(Ni_{0.5}Zn_{0.5})_2Fe_{16}O_{27}$ [Kakuk *et al.*, 2008], ceramics materials Cr_3C [Ko *et al.*, 1997] and TiC [Deevi, 1991] etc. have been reported using SHS process.

2.2.8 Conventional Ceramic Route/Solid State Reaction/High Energy Ball Milling

Conventional ceramic route, also known as solid state route or high energy ball milling route, is the simplest and easily scalable process to produce phase pure ferrites and ferroelectric materials having relatively simple stoichiometric composition e.g. $Ni_{1-x}Zn_xFe_2O_4$ [Islam *et al.*, 2012], $BaTiO_3$ [Manzoor and Kim, 2007] etc. The process involves the mechanical activation of initial raw precursors, generally taken in the form of metal oxides or carbonates by dry milling through ball-mill/grinder/analytical mill etc. Subsequently, the homogenized powder is wet-milled in volatile solvents medium e.g. acetone, ethanol to initiate the homogenization and grain interaction among the precursors. The obtained precursor slurry is dried under normal ambient conditions, which is calcined at optimized temperature for solid state reaction of the constituents to get desired phase of materials. Further, crushing of heat treated lumps is carried out using planetary mill and finally, sieving is done to get the desired size distribution of phase pure material. Solid state reaction route provides the end product by the direct reaction in a simple

single step process using low cost raw precursors, avoids possibility of any impurity phase formation in intermediate process steps. However, there are associated challenges to achieve the stoichiometric composition in final end product. Variety of metal oxides viz. ZnO, In_2O_3, Bi_2O_3, and SnO_2 [Patil *et al.*, 2014], multiferroic $BiFeO_3$ [Suresh and Srinath, 2014], ferroelectric ceramics $PbZr_{1-x}Ti_xO_3$ [Kumari *et al.*, 2014] were reported by solid state reaction route.

2.3 History of Development of Radar/Microwave Absorbing Materials

The research on microwave/radar absorbing materials started in 1930's and the first patented product came in 1936 from Netherlands, made of carbon black and TiO_2 for MW absorption at ~2 GHz. The demand for these products strengthened due to use of radars during World War II. German Scientists [Schade, 1945; MacFarlane, 1945] developed "Wesch" material. consisting of rubber impregnated with carbonyl iron for absorption at ~3 GHz region and 3" thick multilayer absorber using resistive gradient sheets for wide band (~ 2-15 GHz) MW absorption (< -20dB) in submarines. Commercialization of MW absorbing products started in 1950's with a product "Spongex" by M/s Sponge Products Company, consisting of carbon coated animal hair. The product shows -20dB attenuation over 2.4-10 GHz at normal incidence. Later on, the same company tied up with renowned MW product manufacturer M/s Emerson and Cuming, USA. In US, Halpern Anti Radar Paints (HARP) were developed for the airborne and shipboard stealth applications. The airborne version MX-410 was made of well oriented aluminum flakes and carbon black in rubber matrix. This material showed the MW absorption ~ -15 to 20 dB over X-band. Whereas, the ship version was made of iron particles loaded in rubber medium to demonstrate the absorption in X-band frequencies [Montgomery *et al.*, 1948; Halpern *et al.*, 1960]. Similarly, Dallenbach layer, as discussed in section 2.1.3, was developed using a homogeneous lossy layer on metallic substrate with impedance matching at top surface of absorber structure [Ruck *et al.*, 1970]. Around the same period, Salisbury screens, as a resonant absorber, were fabricated using a resistive sheet at quarter wavelength distance from the top and filled with low dielectric spacer as shown schematically in Figure 2.8 [Salisbury; 1952]. Most of the absorbers developed in the initial phases were designed for MW absorption in narrow frequency range, having resonant characteristics. However, with the gradual progress of radar systems and threat perception for military airborne objects in multi-bands of MW spectrum, the need for the development for broad-band stealth products became essential. At that time, the main application of broad band absorbers was to reduce of MW clutters during antenna measurements and in anechoic chambers. The originally developed Salisbury screens, which were showing resonant MW absorption behavior, were modified by inserting few additional spacers and resistive sheets layers to realize the enhanced microwave absorption in the desired frequency regions [Emerson, 1973].

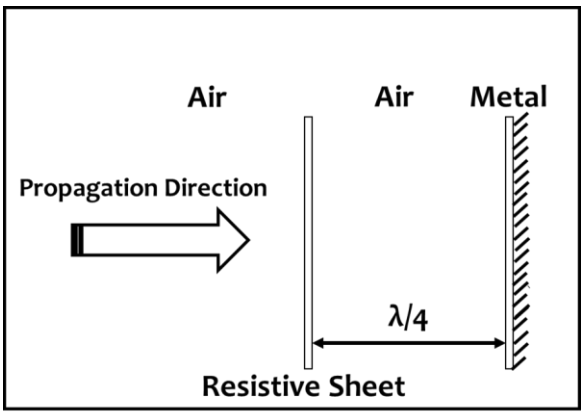

Figure 2.8 : Scheme for Salisbury Screen (Source: Vinoy and Jha, 1996)

The first systematic approach for a broad band MW absorption was realized with the development of Jaumann absorbers, which is designed by placing the stakes of resistive sheets

at λ/4 distance from metallic back substrate and spacer filled in the gap as shown schematically in Figure 2.9 [Severin, 1956]. Further, improvements in microwave absorbers were achieved by fabricating resistive sheets with effective impregnation of carbon powder in organic binder resin and polyethylene as spacer materials to enhance the performance of Jaumann absorbers [Connolly and Luoma, 1977].

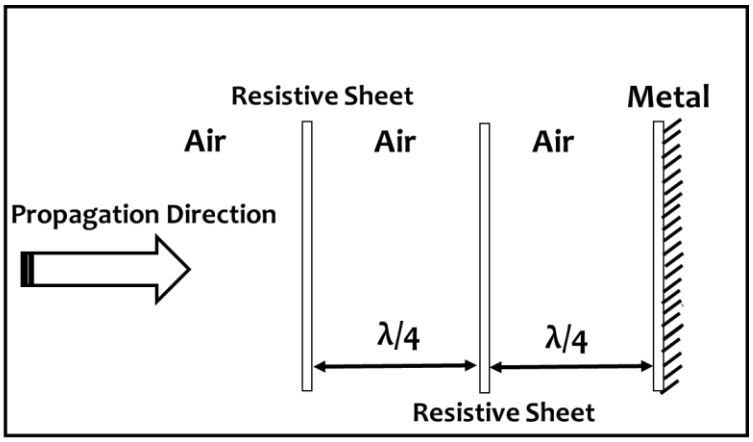

Figure 2.9 : Scheme for Jaumann absorber (Source: Vinoy and Jha, 1996)

Foam based pyramidal bulk absorbers were made of pointed tip with gradual variation of impedance in the structure. These were designed in such a way that incident MW signals encounter maximum attenuation while propagating in the conical structure [Salati, 1954; Tanner 1961]. These absorbers were developed by integrating the pyramid shaped urethane foam structures in conducting slurry of carbonaceous materials. Figure 2.10 shows the absorption scheme in such pyramidal shaped MW absorbers. Further, mat shaped structures were also used in place of foams to control the conductivity of absorbers. These mat shaped structures were made of animal hairs in conducting carbonaceous matrix. These MW absorbing products showed MW reflection losses ~ -40 dB to -60 dB. These materials were developed for use in anechoic chambers and outer antenna measurement systems widely.

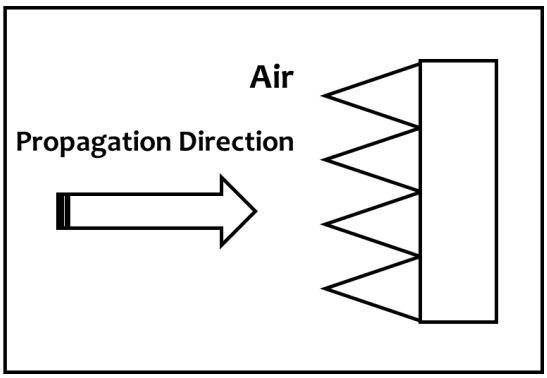

Figure 2.10 : Foam based broad band MW absorbers (Source: Vinoy and Jha, 1996)

During late 1950s, circuit analog radar absorbing materials (CA-RAM) came into existence for MW absorption applications. These materials were designed by depositing the conducting ink on non-lossy sheets having various geometrical patterns as shown in Figure 2.11. This material is used as an alternative of resistive sheet in Salisbury screen for impedance matching. These patterns are analogous to circuit elements viz. resistance, conductance and impedance as shown in Figure 2.11(a). The pattern thickness is a deciding factor for the overall resistance of the circuit and shape and sizes of patterns are the deciding factors for the inductance and capacitance. By optimizing the pattern type and their arrangement, the impedence of layer could be tuned for enhanced reflection losses.

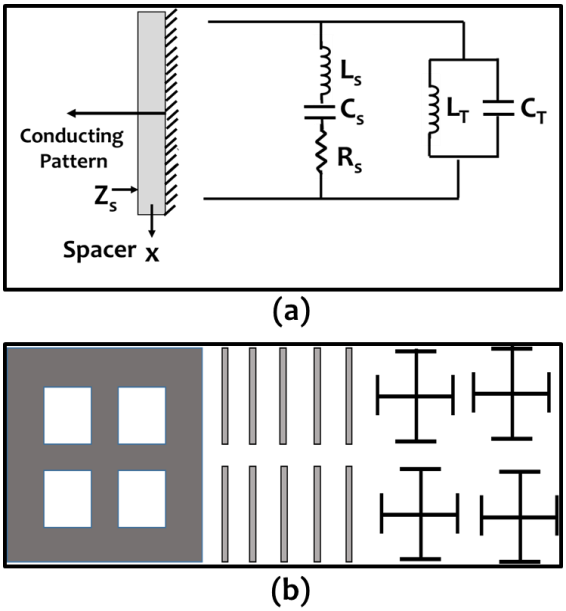

Figure 2.11 : (a) Scheme for circuit analog RAM and its equivalent circuit elements (b) some standard circuit analog geometries in form of rectangular slots, diploes, Jerusalem crosses etc. (Source: Vinoy and Jha, 1996)

Magnetic MW absorbers gained interest due to their absorption capabilities at lesser thickness in the lower frequency bands. The ferrites were widely explored in 1960s and onwards due to their tunable MW absorption properties [Crispin and Siegel, 1968]. The ferrite based layer was used as under layer in CA-RAM for reducing absorber thickness further [Suetake, 1971]. Similarly, honeycomb and mash shaped structures were filled/coated with carbon particles to enhance absorption [Stubbs *et al.*, 1981]. The Jaumann absorber's MW absorption frequency bandwidth was enhanced by including the graded structures [Nortier, *et al.*, 1987].

2.4 Ferrite based Magnetic Materials

Ferrites are mixed valent transition metal oxides, showing ferrimagnetic behavior in general. Initially, efforts were made by Snoek and his group in Philips Research Laboratory, Holland during 1933-1945 for the development of ferrites as commercial viable MW absorber materials [Snoek, 1947; Neel, 1948]. Based on the arrangement of the atoms in crystalline lattice, the ferrites are classified in three types namely spinel, hexagonal ferrites and garnets [Viswanathan and Murthy, 1990]. Ferrite materials attracted the interest of researchers for development of industrial product due to their unique properties e.g. good magnetic permeability, tunability of ferromagnetic resonance (FMR), high electrical resistance, temperature stability, non-corrosiveness, scalability and easy processing [Augustein *et al.*, 1993; Li *et al.*, 2011]. Depending upon the category of ferrites and their composition, they show a range of electrical, magnetic and other physical properties. The different classes of ferrites show different magnetic properties and thus, interact differently with of the incident EM spectrum in different frequency bands. The ferrites, which absorb incident electromagnetic waves, are widely used in the stealth technology for aircrafts. Apart from the composition, the physical properties of ferrites are also highly dependent on methods of preparation, processing conditions viz. sintering temperature and duration, substitution of different cations, grain size, morphology, grain distribution etc. [Smith and Wijnn, 1959]. One of the important criteria for selecting the absorbing material is the location of its natural ferromagnetic resonance (FMR) region. The absorption frequency of a magnetic material will depend on the electron spin in the bulk as well as on the domain spin orientations. Different types of ferrites are developed to explore the resonance absorption over a broad range of frequencies. In the present study we have focused on spinel phase Ni-Zn ferrite system for MW absorption applications over 2-12.4 GHz and cobalt substituted strontium hexaferrites for absorption over 8-18 GHz.

2.4.1 Ni-Zn Spinel Ferrites and their composite Systems

The spinel phase $Ni_{1-x}Zn_xFe_2O_4$ ferrite systems have been explored widely due to the scope of tailoring their physical properties by substituting Zn^{2+} in $NiFe_2O_4$ crystal lattice. Snoek reported for the first time the significant magnetic properties of Ni-Zn ferrites [Snoek, 1947]. Afterwards, the extensive work has been done to explore the MW absorbing applications of Ni and Ni-Zn ferrite systems. The brief outcomes of the major findings are listed in the Table 2.1.

Table 2.1 : Literature review for synthesis of MW absorbing Ni-Zn spinel ferrites and their composites

S. No.	Powder Synthetic Route	Composite Preparation	MW Frequency Range	Majors Findings	References
1.	Low temperature solid state route	$Ni_{0.7}Zn_{0.3}Fe_2O_4$/epoxy resin (60-80 wt% loading)	8-12 GHz	Maximum R.L. ~-21 dB at 10.2 GHz with band width of 2 GHz.	Amiri *et al.*, 2011
2.	Citrate precursor method	$Ni_{1-x}Zn_xFe_2O_4$ (x=0.2, 0.4 and 0.5) ferrite/ epoxy resin(50-80 wt% loading)	8-12 GHz	$Ni_{0.5}Zn_{0.5}Fe_2O_4$ ferrite sample show maximum loss tangent $\tan\delta_m$ ~5.57 at 9.36 GHz with 80wt% loading	Verma *et al.*, 2003
3.	Citrate precursor method	$Ni_{0.5}Zn_{0.5}Fe_2O_4$ ferrite/ epoxy resin	8-12 GHz	Maximum R.L. ~-15 dB at 12 GHz	Lima *et al.*, 2008
4.	Hydrothermal synthesis	$NiFe_2O_4$ ferrite/ paraffin wax	8-18 GHz	R.L. ~ -24 dB at 9.5 GHz and 12.5 GHz (Dual absorption peaks) with MW absorption bandwidth ~ 4.5 GHz	Zhu *et al.*, 2011
5.	Polymer assisted hydrolysis	Ni-Zn ferrite/PEG (Pentaerythritol tetra-polyethylene glycol ether) polymer	1-8 GHz	Maximum R.L. > -20 dB at 1.35 GHz	Shimba *et al.*, 2011
6.	Conventional ceramic route	Ni-Zn ferrite/-Carbon Black (CB) /Polyurethane (PU) resin	8-12 GHz	~4dB MW attenuation over X-band	Dias *et al.*, 2011
7.	Polyacrylamide gel method	$Ni_xZn_{1-x}Fe_2O_4$ (x=0,0.2,0.5, 0.8, 1) pure powders	8.2-11 GHz	R.L. ~ -2.2 to -4.5 dB in the frequency range	Ma *et al.*, 2008
8.	Commercially available Ni-Zn ferrite (Source: MK Impex Corp Canada)	$Ni_{0.5}Zn_{0.5}Fe_2O_4$ ferrite/ CB / PU resin compound coated on cotton fabric	8-18 GHz	Maximum R.L. ~-22.5 dB at 13.5 GHz and R.L. > 7.5 dB over entire band of 12-18 GHz.	Gupta *et al.*, 2014

9.	Sol-Gel Route	$Ni_{1-x}Zn_xFe_2O_4$ ($0 \leq x \leq 1$, in steps of 0.1)/ paraffin wax	1-14 GHz	$Ni_{0.5}Zn_{0.5}Fe_2O_4$/ wax composite sample show maximum R.L. ~-29.6 dB at 6.5 GHz with MW absorption bandwidth ~ 6 GHz	Zhang *et al.*, 2013
10.	Conventional Ceramic route	$Ni_{0.33}Zn_{0.67}Fe_2O_4$/ Polyvinylchloride (PVC) (47.5-73.1 vol.% loading)	01 MHz-01 GHz	R.L. > -20 dB at 0.925 GHz with 47.5 vol.% loading	Dosoudil *et al.*, 2006
11.	Co-precipitation method	$Ni_{0.5}Zn_{0.5}Fe_2O_4$/ Cobalt flakes nanocomposite	1-14 GHz	Maximum R.L. ~ -33.8 dB at 11.5 GHz with band width of 4.5 GHz	*Yan et al.*, 2012
12.	Hydrothermal route	$Ni_{0.5}Zn_{0.5}Fe_2O_4$ ferrite/ Polyaniline(PANI) nanocomposite	2-18 GHz	Maximum R.L. ~ -17 dB at 11.1 GHz with band width of 5 GHz	*Wang et al.*, 2013

2.4.2 Z-type Strontium Hexaferrite and its Composites

Hexaferrites are complex compounds, consist of mainly Ba/Sr along with divalent transition metal ions such as Ni, Co, Mn, Zn, Fe etc. Hexagonal ferrite gained attention among scientific community due to their high magnetic permeability, uniaxial and planar anisotropy and FMR in the GHz range which can be tuned for high frequencies. These materials are mainly utilized for high frequency applications e.g. data storage, magnetic recording, components of electrical devices, EM wave absorbers etc. [Surig *et al.*, 1993; Shams *et al.*, 2008; Sugimoto *et al.*, 2005; Kim and Kim, 2010]. Depending on the lattice arrangements of magneto-plumbite cell, hexaferrites show different crystallographic phases such as M (Ba or $SrFe_{12}O_{19}$), W ($BaMe_2Fe_{16}O_{27}$), Y ($Ba_2Me_2Fe_{12}O_{22}$), Z ($Ba_3Me_2Fe_{24}O_{41}$), X ($Ba_2Me_2Fe_{28}O_{46}$) and U ($Ba_4Me_2Fe_{36}O_{60}$) (where Me is divalent cation mentioned above) with respective ascending structural complexities [Puller, 2012]. Firstly, the M-phase barium hexaferrite materials were developed by Went et al. in Philips laboratory [Went *et al.*, 1951]. Further, more complicated hexaferrite systems, containing both Fe^{2+} and Fe^{3+} species and ternary system were synthesized by researchers [Wijn, 1952; Braun, 1952; Smit *et al.*, 1959].

Among different hexaferrite crystallographic phases, the Y-phase hexaferrite is the only phase, showing planner magnetic anisotropy. However, the Z-type hexaferrite ($Ba_3/Sr_3Me_2Fe_{24}O_{41}$) exhibits conversion of axial anisotropy into planar magnetic anisotropy with cobalt substitution [Smit and Wijn, 1959]. Co-substituted Z-type Strontium hexaferrite ($Sr_3Co_2Fe_{24}O_{41}$) has attracted much attention in recent years due to its high frequency dependent properties and c-axial crystal grain alignment towards easy magnetization direction. The complex geometrical structure of Z-type hexaferrite and simultaneous co-existence of different crystallographic phases poses challenges for synthesis of crystallographically phase pure material [Takada *et al.*, 2006]. In addition, the stoichiometric control of chemical composition is another challenge for such materials. Detailed literature survey has been carried out on reported synthesis techniques to obtain pure Z-phase material. However, no specific report was found on MW absorption properties of Z-type Co substituted hexaferrites. The Table 2.2 briefly summarizes the work carried out in this direction.

Table 2.2 : Literature review for synthetic route for pure Z-type Ba/Sr hexaferrite powders

S. No.	Synthetic Route	Processing Conditions	Key Studies Undertaken	Major Findings	References
1.	Sol-gel precursor route	Annealing at 1200°C/3h	Established synthesis route	Observed saturation magnetization M_s ~ 48.5 emu/g	Pullar and Bhattacharya, 2001
2.	Solid state precursor route	Sequential heating in air and oxygen ambient	Magneto-electric effect	Oxygen sintered $Sr_3Co_2Fe_{24}O_{41}$ showed low-field magnetically induced ferroelectric properties.	Kitagawa *et al.*, 2010
3.	Co-precipitation technique	Sintering in the range of 1100-1300°C for 14 h	Frequency and field dependent permeability studies	Co_2Z was found to be suitable for device application due to high permeability >5 for MW L-band applications	Daigle *et al.*, 2012
4.	Polymerizable complex method	Heating at 1473 K for 5h in air	Magnetic properties	Observed saturation magnetization M_s ~50.5 emu/g	Kikuchi *et al.*, 2011
5.	Conventional ceramic route	Combination of Ba and Sr divalent ions in chemical composition. Sintering at 1050°C for 3h	Magnetic and microwave antenna studies	With increase of Sr content M_s increases. At optimized Sr concentration the permeability >7.5. Z-phase with Sr content showed better properties as compared to Sr free composition.	Xinag *et al.*, 2011
6.	Co-precipitation technique	Heat treatment in the range of 500-1250°C for 2h	To establish synthetic routes for getting pure Z-phase	Pure Z-phase of Ba prepared by reaction of M and Y-phases.	Hsiang and Yao, 2007
7.	Citrate precursor method	Heat treatment in the range of 20-1000°C for 4h with heating rate 10°C /min.	Microwave absorbing applications	$Ba_3Co_{0.9}Cu_{1.1}Fe_{24}O_{41}$/ polychloroprene composite exhibit maximum R.L. ~ 22.5 dB at 9.5 GHz	Caffarena *et al.*, 2007
8.	Solid state precursor route	Sequential heating in the range of 1100-1450°C for 2-12h duration.	Permittivity and permeability studies	Co_2Z was found to be suitable for antenna applications due to high permeability >9.5 at 1 GHz	Hill, 2013

9.	Co-precipitation technique	Two stage heat treatment in the range of 900-1350°C	Return Loss studies in the range of 100MHz-1 GHz	R.L. ~-12 dB at 0.8 GHz	Ryu *et al.*, 2011
10.	Co-precipitation technique	Heat treatment in the range of 800-850°C for 2-4h	Magnetic properties	Observed saturation magnetization M_s> 60 emu/g	Robert and Mari, 1992
11.	Hydrothermal route	Heat treatment at ~800°C for 1h	To establish synthetic routes for getting pure Z-phase	Pure Z-phase ferrite prepared by heating for short duration	Mueller *et al.*, 1991
12.	Solid State Precursor route	Sequential heating in air and oxygen ambient	Magneto-dielectric studies	Negative Magneto-dielectric effect was observed in Z-type Sr hexaferrite composition	Zhang *et al.*, 2012

2.5 Core-Shell Nanomaterials and their Composites

Nanoscale materials show promise due to their unique physical/chemical properties for the development of various present and future specialized technologies and applications [Capek, 2006; Ainsworth, 2004]. Inorganic, organic and their composite materials can be synthesized in nanometer geometries with novel chemical, physical and other functional properties, which are usually not found in their bulk counterparts. The composite nanomaterials offer additional property of integrating of other functional properties. For the preparation of composite nanomaterials, polymers have been considered as the excellent host materials to control the size and shape of the nanomaterials. Numerous polymer composite systems have been synthesized with a wide variety of inclusions like metals and semiconductors, carbon nanotubes and magnetic nanoparticles [Heilmann, 2003; Muisener *et al.*, 2002]. The synthesis process has led to different geometrical structures, however, among them core-shell structures have gained interest. These materials show structural dependent MW absorption properties due to both the functional role of dielectric shell and magnetic core simultaneously. The dielectric shell eliminates the magnetic coupling of metal nanoparticles [Sugimoto *et al.*, 1998; Sugimoto *et al.*, 2002; Liu *et al.*,2005; Che *et al.*, 2006] and metallic nanoparticles in core have excellent MW absorption capabilities due to their quantum effects, low density, high saturation magnetization and enhanced Snoek's limit [Snoek, 1947; Diandra and Reuben, 1996; Bregar, 2004]. To enhance the interaction of core nano-metal with the external field, the shell thickness needs to be less than the skin depth [Xie *et al.*, 2011]. Nanostructured materials with variety of magnetic cores and different classes of dielectric shells e.g. Fe/SmO, Fe/ZnO, FeCo/Al_2O_3, Co/Y_2O_3 etc. [Liu *et al.*, 2008; Liu *et al.*, 2009] studied by different research groups due to their capabilities of tuning both relative permittivity and permeability values. However, core-shell structures, having nanocrystalline magnetic metal and carbonaceous shell, are found to be superior not only due to the excellent interfacial polarization but also due to the good dielectric loss properties in MW region [Han *et al.*, 2009; Lian *et al.*, 2007; Liu *et al.*, 2003]. Based on the nature of inner core nanometals, the encapsulated carbon may have different phases viz. amorphous, polycrystalline or graphitic. Among them, the graphite encapsulated nanometal core-shell structure are considered relatively superior due to their improved dispersion properties in the host matrix while making rubber based composite materials. The following Table 2.3 is summarizing the work on carbon/graphite coated magnetic nanomaterials and their composites for MW absorption applications

Table 2.3 : Literature review for synthesis of MW absorbing core-shell nanomaterials and their composites

S. No.	Material Details	Synthetic Technique	Composite Preparation	MW Frequency Range	MW Absorption	References
1.	Graphite coated Ni Nano capsules	Arc-discharge method	In paraffin wax matrix (50 wt% loading)	2-18 GHz	Maximum R.L. ~ -32 dB at 13 GHz with band width of ~4 GHz.	Zhang *et al.*, 2006
2.	Amorphous carbon coated Fe-Sn metal nano alloy	Wet chemical gel to carbonate route followed by pyrolysis in inert ambient	In NBR matrix (50-80 wt% loading)	8-18 GHz	Maximum R.L. ~ -44 dB at 11 GHz with band width of 10.3 GHz.	Gupta *et al.*, 2012
3.	Graphite coated Fe Nano capsules	Arc-discharge method	In paraffin wax matrix (50 wt% loading)	2-18 GHz	Maximum R.L. ~ -43.5 dB at 9.6 GHz with band width of ~3 GHz.	Zhang *et al.*, 2007
4.	Graphite coated Fe metal nanoparticles	Wet chemical gel to carbonate route followed by pyrolysis in inert ambient	In NBR matrix (50 and 80 wt% loading)	8-12 GHz	Maximum R.L. ~ -41 dB at ~12 GHz with band width of 2 GHz.	Gupta *et al.*, 2014
5.	Graphite coated Fe/Ni metal nanoparticles	Arc-discharge method	In paraffin wax matrix (50 wt% loading)	2-18 GHz	Maximum R.L. ~ -47.3 dB at 9.6 GHz with band width of ~2 GHz.	Lu *et al.*, 2008
6.	Graphite coated Fe-Ni metal nano alloy	Arc-discharge method	In paraffin wax matrix (40 wt% loading)	12.4-18 GHz	Maximum R.L. ~-26.9 dB at 16 GHz with band width of ~6.6 GHz over Ku-band	Liu *et al.*, 2009
7.	Graphite coated Fe-Ni metal nano-alloy	Arc-discharge method	In paraffin wax matrix (40 wt% loading)	12.4-18 GHz	Maximum R.L. ~ -14 dB at14 GHz with band width of ~9 GHz over Ku-band	Liu *et al.*, 2010
8.	Ni/(C,N) nano capsules	Modified Arc-discharge method	In paraffin wax matrix	2-18 GHz	Maximum R.L. ~-35 dB at 13.6 GHz with band width of ~2 GHz	Wu *et al.*, 2010

2.6 PEROVSKITE OXIDE MATERIALS

Perovskite oxides are crystalline dielectric ceramics, having general stoichiometric formula ABO_3.These oxide systems were first discovered by Gustav Rose in 1839. In such ABO_3 perovskite type oxide systems, A site is occupied by large alkaline earth metal cation (e.g. Pb, Bi, Ba, Sr, Zr, Li etc.), coordinated by 12 oxygen ions, whereas B site is occupied by transition metal ions (Fe, Co, Mn, Ti, Ta, W, Nb etc), coordination with 6 oxygen ions [Zhu *et al*., 2014]. Perovskite oxides are advantageous over the conventional ceramic materials as the compositional variation at A and B sites can be tailored without affecting the crystallographic phase and basic properties of materials [Grabowska, 2016; Khamoushi, 2014]. Dielectric properties of these materials are decided by the onset of polarization and alteration of dipoles due to thermal expansion at A and B sites [Steenwinkel *et al.*, 2007; Setter *et al*., 1994; Ivanov *et al*., 1998]. Further, due to tunable dielectric properties, these materials may have potential for microwave absorbing applications. However, very few report are available on MW absorption of perovskite materials [Alvarez *et al*., 2011; Panwar and Puri, 2016; Sobiestianskas *et al*., 2012]. Various perovskite oxides viz. $PbTiO_3$, $KTaO_3$, $SrTiO_3$, $PbZr_{1-x}Ti_xO_3$, $LiNbO_3$ etc. have been widely studied by different research groups for their applications in actuators, transducers, MEMS, thermistors, FET devices, Multilayer Ceramic Capacitors (MLCs) etc. [Bhattacharjee and Pandey, 2011; Jaffe *et al.* 1971; Vijatovic *et al*. 2008; Ertug, 2013]. In the present study, we considered simple $BiFeO_3$ and $BaTiO_3$ perovskite systems, having multiferroic and ferroelectric properties, which make them suitable materials for MW absorption.

2.6.1 Tetragonal Phase Barium Titanate ($BaTiO_3$) Ferroelectric and its Composites

Ferroelectrics are class of materials, having structure dependent polarization effects with a possibility to tune their dielectric properties. These materials have spontaneous polarization along with field dependent reorientation, making them suitable for microwave absorption application. Among the ferroelectric materials, $BaTiO_3$ is the first perovskite oxide discovered with ferroelectric properties by E. Wainer and A.N. Salomon [Wainer and Salomon; 1942]. The Curie temperature for $BaTiO_3$ is 130°C, above which the material exhibits cubic crystallographic state whereas below this temperature it converts into tetragonal phase [Park et al., 2006]. The onset of ferroelectric properties in such system induces dipole relaxation, useful for MW absorption. The previous work done on $BaTiO_3$ related ferroelectric systems and its composites for MW absorbing application is summarized in Table 2.5 below:

Table 2.5 : Literature review for synthesis of MW absorbing $BaTiO_3$ and its composites

S. No.	Powder Synthetic Route	Composite Preparation	MW Frequency Range	MW Absorption	References
1.	Wet chemical hydrothermal route	In paraffin wax matrix (40-60wt% loading)	0.5-15 GHz	Maximum R.L. ~ -21.8 dB at 15 GHz with band width of ~ 1.7 GHz	Zhu *et al.*, 2012
2.	Sol-gel method	In epoxide resin (2-8 Vol % loading)	8-18 GHz	Maximum R.L. ~ -18 dB at ~ 13 GHz with band width of ~ 3.5 GHz	Chen *et al.*, 2007
3.	Solid state reaction	$BaTiO_3$-Polyaniline composite in PU resin matrix (50 wt% loading)	8-12 GHz	Maximum R.L. ~ -15 dB at ~ 10 GHz with band width of ~ 3 GHz	Abbas *et al.*, 2005
4.	Solid state route	$BaTiO_3$- carbonyl iron composite in epoxy	2-18 GHz	Maximum R.L. ~ -59 dB at ~ 12.5 GHz with band width of ~ 4 GHz	Qing *et al.*, 2011

		resin (20, 50 wt% loading)			
5.	Sol-gel method	In PU resin matrix (50-90 wt% loading)	8-18 GHz	Maximum R.L. ~ -27 dB at ~12 GHz with band width of ~ 10 GHz	Jain *et al*., 2013
6.	Sol-gel method	In paraffin wax matrix (70 wt% loading)	2-18 GHz	Maximum R.L. ~ -29.6 dB at ~12 GHz with band width of ~ 1.5 GHz	Jing *et al*., 2009
7.	Wet chemical hydrothermal route	In epoxy resin matrix (50 wt% loading)	8-18.5 GHz	Maximum R.L. -40.4 dB at 14.6 GHz with band width of ~ 2.7 GHz	Murugan *et al*., 2010

2.6.2 Bismuth Iron Oxide ($BiFeO_3$) Multiferroic and its Composites

Multiferroics are a class of materials with coupled electric, magnetic, and structural order parameters, resulting into simultaneous onset of ferroelectricity, magnetism, and ferroelasticity in the single phase material [Salje *et al*., 1990]. The multiferroic systems offer advantages over conventional magnetic and ferroelectric materials because of the magneto-electric coupling between ferroelectric and magnetic ordering in a single phase of such material, which may lead to the enhanced frequency region for MW absorption applications. These materials exhibit contradictory physical characteristics of both magnetic and ferroelectric ordering in single phase material (where magnetic ordering requires unfilled d/f orbitals and ferroelectric ordering demands d_0 or completely filled d orbitals) [Pradhan *et al.,* 2005; Layek and Verma, 2012]. The weak ferromagnetic behavior of multiferroic materials like $BiFeO_3$, above room temperature, may show the phenomenon of magnetic relaxation in conjunction with dielectric/ferroelectric relaxation. This behavior may assist in better absorption of microwave radiation. However, the material suffers from the oxygen vacancies and impurities phases such as Bi_2O_3, $Bi_2Fe_4O_9$ etc., which hamper the EM absorption properties [Wang *et al.,* 2004; Kumar *et al*., 2000]. To overcome this problem, efforts have been made to explore the new synthesis routes and pre/post annealing profiles to optimize the synthesis process for single phase $BiFeO_3$ in bulk and nano geometries [Freitas *et al.*, 2013]. The work done on MW absorbing properties BiFeO3 system is summarized in Table 2.4 below

Table 2.4 : Literature review for synthesis of MW absorbing $BiFeO_3$ and their composites

S. No.	Synthetic Route	Processing Conditions	MW frequency	MW Absorption	Reference
1.	Sol-gel method	Calcination at 300°C and post-sintering at 500°C for 2h	12.4-18 GHz (Ku-Band)	Maximum R.L. ~-26 dB at 16.3 GHz with band width of ~ 4.9 GHz	Kang *et al*., 2009
2.	Citrate based Sol-gel method	Heating in the range of 600-700°C for 1h	8.2-12.4 GHz (X-Band)	Maximum R.L. ~ -46 dB at ~8.4 GHz with band width of ~ 2.5 GHz	Sowmya *et al*., 2015
3.	Sol-gel followed by high pressure synthesis	Annealing at 800°C under high pressure ~ 5GPa conditions	1-18 GHz	Maximum R.L. ~ -17 dB at ~11.2 GHz with resonating behavior	Wen *et al*., 2015
4.	Sol-gel method	Calcination at 300°C and post-sintering at 500°C for 2h	8.2-12.4 GHz (X-Band)	Maximum R.L. ~ -20 dB at ~10.8 GHz with band width of ~ 2 GHz	Li*et et al*., 2015

2.7 PREPARATION OF MW ABSORBING RUBBER COMPOSITES

The functional MW absorbing materials in powder form cannot be used directly on military and civil targets for their real time application. For actual applications of these materials, a suitable host matrix and processing methodology need to be identified and developed, to convert the powder materials into a finished product in the form of coatings/sheets/structures. The dispersion of filler materials in the insulating matrix gained interest since the thrust of commercialization of these products for MW absorption applications. Various host matrices viz. polymer [Raju and Murthy, 2013; Yang *et al.*, 2011; Dosoudil *et al.*, 2008], resins [Nanni, *et al.*, 2009], wax [Bueno *et al.*, 2008], glass/epoxy [Oh *et al.*, 2004; Chin and Lee, 2007], elastomers [Zou *et al.*, 2011; Feng *et al.*, 2007; Meng *et al.*, 2009], fabrics [Gupta *et al.*, 2014; Park *et al.*, 2006], ceramics etc. have been used to impregnate different classes of MW absorbing filler powders. The studies on the composite materials are mainly emphasized on the loading of filler material into the host matrix, distribution/ dispersion of material's granules into a medium, their effect on EM properties and the optimization of MW absorption characteristics. Further, the shape, size, distribution and interaction of filler particles, which act as MW scattering centers, affect the MW absorption properties [Singh *et al.*, 2012]. Therefore, selection of a proper host matrix, its processing for uniform dispersion of filler materials, to maintain the uniform thickness of composite, shaping/forming of final products etc. are important for real time applications. However, in practice numerous difficulties are being faced during preparation of homogeneous filler-host matrix composites e.g. non-uniform distribution of heavy ceramic particulates in resins mediums due to the settling issues of high density filler materials, un-even suspension of filler powders in wax/polymeric matrix due to limitation of processing techniques, difficulties in heavy loading of light weight carbonaceous materials in matrix due to high volume/weight ratio etc. Further, these process parameters affect the functional, mechanical and environmental properties of the final product. To counter these challenged/difficulties, in the present thesis work, elastomeric matrix has been selected due to its following advantages over other systems:

- Better dispersion of filler materials through the entrapment of filler particles in cross linked vulcanized rubber matrix.
- Excellent mechanical and environmental characteristics due to processing of rubber with other ingredients for their improvement
- Custom moldability of rubber sheets in any shape, size and thickness.
- Elongation and flexibility of final rubber product for their application on any shape of targets

2.8 IDENTIFIED GAPS

A comprehensive review has been presented for the different types of microwave absorbing materials, including synthesis methods and MW absorption properties for different materials in previous sections. Further, for any real usability of these materials on actual targets, their present status has also been reviewed at national and international level for the fabrication of MW absorbing products (coating/sheets/structures). It has been observed that various research groups are working for the development of MW absorbing materials and products. From the forgoing discussions, we find that there are still certain technological gaps and challenges, which limit their real time applications. Some of these challenges and technology gaps are:

(i) Exploration of scalable synthetic routes for the preparation of microwave absorbing materials in larger quantity to meet the requirement for their large area application on actual targets and cost effectiveness.

(ii) Tunability of EM properties of materials over the desired wide frequency bands by compositional variation.

(iii) Identification of processing technology to transform materials into the products, with good functional, mechanical and environmental properties.

(iv) Reduction of thickness and weight penalty of the products for practical application on airborne platforms.

(v) Availability of materials and products for the entire spectrum of MW radiation.

The work presented in the current thesis aims at to bridge some of these technology gaps by way of identification of materials for desired MW frequencies, process optimization of the reproducible synthesis of identified materials and also development of new functional materials. The thesis work emphasized the development of new materials and related products to cover the broad MW frequency bands. The efforts have been made to identify the suitable compositions and materials type with optimum absorption properties. Further, significant thrust has been given to optimize the process parameters viz. chemical compositions, pH conditions, sequential heating cycles etc. in order to get the reproducible MW absorption properties and their rubber based MW absorber products.

2.9 SUMMARY

Microwave absorbing materials are extremely important for the survivability enhancement of airborne military platforms keeping in view the present threat scenario particularly with the advancements in the field efficient radar system for early detection of airborne objects. Such materials are also highly useful for the protection of the instrumentation/human beings with adverse effect of MW radiation. We have presented the basic concepts of MW loss mechanism in dielectric and magnetic materials, in conjunction with the governing parameters and related relations for the optimum absorption. Further, various synthesis techniques for microwave absorbing materials have been discussed, with their advantages and disadvantages in terms of phase/compositional purity, scalability, processing conditions and cost effectiveness for the final product. Further, the historical developments of microwave/radar absorbing products have also been discussed in details including the development of different classes of MW absorbing materials viz. Ni-Zn spinel ferrites, Z-type Sr hexaferrites, graphite coated metal core- shell structures, ferroelectric $BaTiO_3$ and multiferroic $BiFeO_3$ material by different research groups.

...